

# Extinction due to amorphous carbon grains in red quasars from the SDSS

B. Czerny<sup>1</sup>, J. Li<sup>2</sup>, Z. Loska<sup>1</sup>, R. Szczerba<sup>3</sup>

<sup>1</sup>*Copernicus Astronomical Center, Bartycka 18, 00-716 Warsaw, Poland*

<sup>2</sup>*Great Neck North High School, Great Neck, NY, 11024, USA*

<sup>3</sup>*Copernicus Astronomical Center, Rabiańska 8, 87-100 Toruń, Poland*

5 November 2018

## ABSTRACT

We construct a quasar extinction curve based on the blue and red composite quasar spectra of Richards et al. (2003) prepared from the SDSS survey. This extinction curve does not show any traces of the 2200 Å feature characteristic of the Interstellar Medium, and this indicates that graphite grains are likely absent close to quasar nuclei. The extinction is best modeled by AC amorphous carbon grains, assuming a standard distribution of grain sizes ( $p = 3.5$ ) but slightly larger minimum grain size ( $a_{min} = 0.016\mu\text{m}$ ) and lower maximum grain size ( $a_{max} = 0.12\mu\text{m}$ ) than the respective canonical values for the interstellar medium. The dust composition is thus similar to that of the dust in AGB stars. Since graphite grains form from amorphous carbon exposed to strong UV irradiation the results indicate that either the dust forms surprisingly far from the active nucleus or in a wind that leaves the nucleus quickly enough to avoid crystallization into graphite.

**Key words:**

## 1 INTRODUCTION

It is well known that the spectra of Seyfert galaxies – particularly Seyfert 2 galaxies – are considerably modified by circumnuclear extinction. It is also believed that Narrow Line Seyfert galaxies are on average redder than typical Seyfert 1 galaxies because of reddening due to the presence of dust (e.g. Kuraszewicz & Wilkes 2000, Constantin & Shields 2003). Evidence is now accumulating that a significant fraction of bright AGN, including high redshift quasars, are affected by dust.

The dust is seen directly in emission (IR continuum of dust and emission lines of accompanying molecular gas; e.g. Priddey et al. 2003, Omont et al. 1996, Kuraszewicz et al. 2003, Andreani, Francheschini & Granato 1999). The presence of dust may also be detected indirectly because of its effect on the quasar continuum in the optical/UV band. Recent surveys show the widespread presence of red quasars in quasar samples, and reddening by dust is the most plausible explanation for their spectral shape (e.g. FIRST quasar sample, White et al. 2003; SDSS quasar survey, Richards et al. 2003; 2MASS red quasars, Marble et al. 2003).

Knowledge of dust properties in the close vicinity of an active nucleus is thus important both for determining intrinsic AGN spectra and understanding the conditions in the gas surrounding the nucleus.

It has already been argued that the properties of the

dust in such extreme conditions need not be similar to the dust properties in the interstellar medium of our Galaxy. It has been found that the extinction curve of Prévot et al. (1984) determined for the Small Magellanic Cloud (SMC) roughly applies to AGN dust (e.g. Czerny, Loska & Szczerba 1991, Laor & Draine 1993, Pitman et al. 2000, Kuhn et al. 2001, Richards et al. 2003).

In this paper we use the composite spectra of quasars from the Sloan Digital Sky Survey (SDSS) prepared by Richards et al. (2003) to determine an observational quasar extinction curve. We then compare this curve with model curves and argue that the circumnuclear regions of AGN are filled with amorphous carbon grains. We provide a simple empirical formula for this new extinction law.

## 2 EXTINCTION CURVE FROM RED SDSS QUASARS

Results from the SDSS were used by Richards et al. (2003) to create 6 composite quasar spectra (see their Fig. 7), selected according to the adopted ranges of the (g-i) color excess. Composite 1, made from 770 objects, contains the bluest quasars in the sample. Their optical/UV slope is well fitted by a power law,  $F_\nu \propto \nu^\alpha$ , with energy index  $\alpha = -0.25$ . Composites 1 to 4 each consist of 770 objects. Composite 5

arXiv:astro-ph/0401158v1 9 Jan 2004

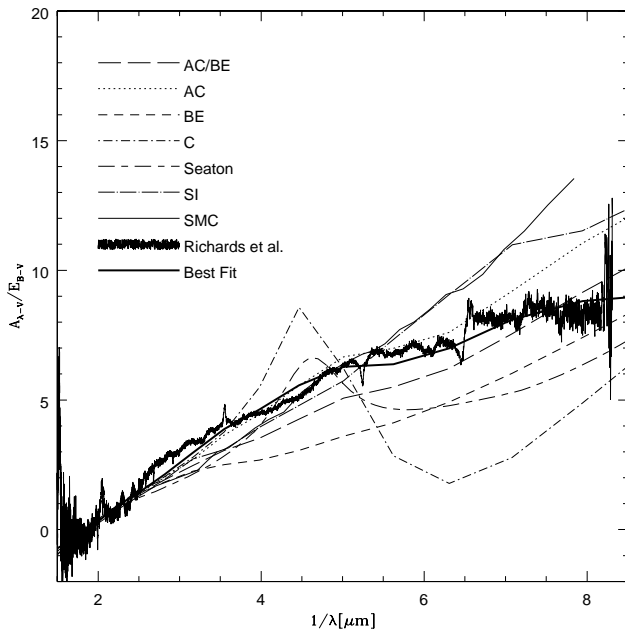


**Figure 1.** The quasar extinction curve (Richards et al. line) derived assuming that composite 1 represents the intrinsic spectrum of all the composites. Seaton and SMC lines show observationally determined extinction curves in the Interstellar Medium (Seaton 1979) and in the Small Magellanic Cloud (Prévot et al. 1984). The Best Fit line shows the favored model extinction curve: AC amorphous carbon grains,  $a_{min} = 0.016\mu\text{m}$ ,  $a_{max} = 0.12\mu\text{m}$ ,  $p = 3.5$ . Other lines show typical model extinction curves obtained assuming the grain distribution characteristic of the interstellar medium ( $a_{min} = 0.005\mu\text{m}$ ,  $a_{max} = 0.25\mu\text{m}$ ,  $p = 3.5$ ) but for different materials (Si - silicates, AC - pure AC amorphous carbon, BE - pure BE amorphous carbon, C - graphite).

consists of 211 objects well representing a red quasar population; only objects with large color excesses were included, but the few reddest objects were rejected in order to preserve the completeness of the sample.

We assume that the bluest composite (composite 1) is essentially unaffected by extinction (we will return to this point in the Discussion). We then assume that other composites intrinsically represent the same spectrum as composite 1, except affected by dust.

We can therefore directly construct the observed quasar extinction curve for each of the composites from 2 to 5 vs. composite 1 by using its usual definition,

$$X(\lambda) = \frac{A_{\lambda-V}}{E_{B-V}} = \frac{A_{\lambda} - A_V}{A_B - A_V}, \quad (1)$$

where

$$A_{\lambda} = 2.5 \log(F_{\lambda}^1/F_{\lambda}^i). \quad (2)$$

Here  $F_{\lambda}^1$  is the composite 1 spectrum and  $F_{\lambda}^i$  is one of the redder composites. The values  $A_V$  and  $A_B$  are calculated at the corresponding visual (5500 Å) and blue (4400 Å) wavelengths.

The curves obtained from composites 2 and 2n were very noisy since the differences between the spectra were small, so we neglected them. We next averaged the curves

obtained from composites 3, 4 and 5 in order to reduce errors, thus creating a single curve.

The resulting extinction curve in the range covered by the SDSS data is shown in Fig. 1. The curve is monotonic with wavelength, without any trace of the 2200 Å absorption feature. It thus resembles the observationally determined extinction curve for dust in the Small Magellanic Cloud (Prévot et al. 1984) more than the Seaton (1979) extinction curve that characterizes the interstellar dust in our galaxy. Accordingly, if the composite spectra are indeed shaped by circumnuclear extinction, the dust composition close to quasar nuclei must be non-standard.

In order to analyze the quasar extinction curve properties, we compare it with several theoretical extinction curves.

### 3 THEORETICAL EXTINCTION CURVES

We construct the model extinction curves for the dust surrounding an active nucleus following the approach of Czerny et al. (1995).

We assume that the nucleus is a source of radiation with a spectral shape given by the sum of two components: a power law component extending from IR to X-rays, and an accretion disc component dominating the optical/UV part. The power law component is spherically symmetric while the disc component intensity depends on the cosine of the inclination angle to the disc symmetry axis.

The innermost part of an AGN is surrounded by a spherical dust shell. The inner radius of the dusty shell is determined by the temperature of dust evaporation. The outer radius of the shell is assumed to be at 300 pc, and the adopted density profile is given in the form of a power law,  $n(r) \propto r^{-0.75}$ , the favored one by models of the far-IR spectra of AGN (e.g. Loska, Szczerba & Czerny 1993, Granato, Danese & Franceschini 1997). The results are not very sensitive to these parameters so long as the spatial distribution is rather flat.

We determine the theoretical extinction curve by solving for the radiation transfer through the dust surrounding the envelope, determining the dust-reddened radiation spectrum, and comparing this spectrum to the intrinsic spectrum of the source, using Eqs. 1 and 2. The radiative transfer is solved for as described by Loska et al. (1993). The temperature of the grains of a given size and chemical composition is calculated from the energy balance. We assume a maximum carbon grain temperature of 1500 K and maximum silicate dust temperature of 1000 K, and we allow for selective grain evaporation close to the inner edge of the dusty cloud. The radiative transfer is solved for assuming that the dust is optically thin, i.e. we neglect multiple scattering effects.

Optical properties of astronomical silicate and carbon grains are taken from Draine (see Laor & Draine 1993), and the amorphous carbon properties were calculated using Mie theory and the optical constants of Martin (see Rouleau & Martin 1991). Some modifications were introduced for large grains/short wavelengths (see Czerny et al. 1995 for details). The distribution of grain sizes was assumed to be in a power law form,  $n(a) \propto a^{-p}$ , with minimum and maximum grain sizes given by  $a_{min}$  and  $a_{max}$ . The standard values of these parameters in the ISM are:  $p = 3.5$ ,  $a_{min} = 0.005\mu\text{m}$  and

$a_{max} = 0.25\mu\text{m}$  (Mathis, Rumpl & Nordsieck 1977). We generally tried to minimize departure from these values.

The extinction curves representing various chemical compositions of dust grains but otherwise based on the dust parameters  $p$ ,  $a_{min}$ , and  $a_{max}$  of the ISM are shown in Fig 1. The observed extinction curve roughly follows at long wavelengths the extinction curve of dust consisting of AC amorphous carbon grains. The departure is seen only at short wavelengths above  $\sim 1500 \text{ \AA}$ .

We can find a better representation of the observed curve assuming AC composition but allowing for a change in the minimum and maximum grain sizes. In Fig. 1 we show such a curve with  $a_{min} = 0.016\mu\text{m}$  and  $a_{max} = 0.12\mu\text{m}$ .

We also analyzed the properties of dust of other chemical compositions, but they did not mimic the quasar extinction curve equally well. In particular, no other standard or non-standard extinction curve could reasonably trace the observational extinction curve in the  $.2\mu\text{m}$  to  $.5\mu\text{m}$  range. Furthermore, we do not expect large amounts of silicates in AGN surroundings; silicate emission features expected in the IR are weak or absent in most AGN (Roche et al. 1991), and efficient formation of CO molecules offers a natural explanation for the depletion of the oxygen necessary for silicate formation (Rawlings & Williams 1989). Any significant contribution from graphite also resulted in the presence of a  $2200 \text{ \AA}$  peak and no traces of such a peak are in the data. We thus argue that AC amorphous carbon grains best describe the observational extinction curve based on the Richards et al. (2003) data because there are significant errors when attempting to model the curve based on any other dust grains.

## 4 DISCUSSION

The lack of the  $2200 \text{ \AA}$  absorption feature due to graphite grains characteristic of interstellar extinction was already noted in several papers concerning AGN (e.g. Pitman et al. 2000, Kuhn et al. 2001, Richards et al. 2003) and therefore an SMC extinction curve seems to apply better than the Seaton ISM extinction curve. Our results based on SDSS quasars from Richards et al. (2003) support this view.

Our best model of the observational quasar extinction curve is made from amorphous AC carbon grains. We assumed a standard power law size distribution of grains,  $p = 3.5$ , but better agreement with the observational curve required a narrower size range (minimum size  $0.016\mu\text{m}$ , maximum size  $0.12\mu\text{m}$ ) than the canonical one of Mathis et al. (1977),  $0.005$  and  $0.25\mu\text{m}$ .

This extinction curve is slightly flatter than the SMC extinction curve at short wavelengths. The reddening law corresponding to it can be well approximated by the following empirical formula

$$\frac{A_\lambda}{E_{B-V}} = -1.36 + 13 \log(1/\lambda)[\mu\text{m}], \quad (3)$$

in the range of  $1/\lambda$  between  $1.5$  and  $8.5 \mu\text{m}^{-1}$ .

Our analysis was based on an average of several observational curves derived from Richards et al. (2003) quasar data. We derived extinction curves assuming that their composite 1 was the intrinsic spectrum of all the composites. We were then able to construct extinction curves based on composite 1 vs. composites 2 through 5 and composite 1n vs.

composites 2n through 5n. We ended up disregarding the composite 1 vs. composite 2 and composite 1n vs. composite 2n extinction curves because they were too noisy. We then averaged the extinction curves based on composite 1 vs. composites 3 through 5. We selected the composite 1 vs. composite 5 extinction curve over the composite 1n vs. composite 5n curve because the former has higher signal-to-noise. The latter was corrected for redshift and magnitude differences, but we found that the two curves were quite similar with the latter having more noise. We did not include the 2n through 5n subgroups in our average because these quasars were already included in the 2 through 5 composites. We found that the composite 1 vs. composites 3 through 5 and composite 1n vs. composites 3n through 5n created a small range of possible extinction curves. We believe that the true observational extinction curve lies somewhere within this range, and so our final observational extinction curve is an average of the curves that are contained in this range. We find that AC amorphous carbon grains are able to model the extinction curves within this range as well as they model the average extinction curve. We also find that even the lower extinction curves in this range are modeled with difficulty when taking into account other types of dust grains.

Our analysis used the composite spectra. Any such spectra, including those of Richards et al. (2003), contain systematic errors which are difficult to assign. The errors come partially from the calibration uncertainty, and partially from the systematic differences in the objects constituting the short wavelength and the long wavelength parts of the final spectrum. Therefore, determination of the errors of the derived extinction curve is rather difficult. Although the conclusion about the dominating role of amorphous carbon seems to be firm, the grain size range needs confirmation.

This dust composition is not surprising taking into account that the conditions around an active nucleus are quite similar to conditions in the envelopes of asymptotic giant branch (AGB) stars. Radiation flux, pressure and densities may be comparable (see e.g. Elvis, Marengo and Karovska 2002), particularly taking into account that the cool gas in AGN is possibly in the form of clouds. This is indicated by the presence of the Broad Line Region and Narrow Line Region implied by AGN spectra. Extinction in carbon-rich AGB stars is also dominated by amorphous carbon, although in some stars with additional silicon carbide (e.g. Piovan, Tantaló & Chiosi 2003).

The  $2200 \text{ \AA}$  feature seen in the interstellar medium is caused by single graphite and/or clusters of graphite grains (see e.g. Draine & Lee 1984, Andersen et al. 2003). Laboratory data indicate that graphite grains form from amorphous carbon grains as a result of exposure to strong UV radiation (Ogmen & Duley 1988; see also Dorschner & Henning 1995). AGN environments provide intensive UV flux, much more than the relatively cool environments of AGB stars (their temperature is of the order of  $2000 - 4000 \text{ K}$ ), yet graphite grains apparently do not form in AGN surroundings. This may support the view of Elvis et al. (2002) that the dust forms in an outflowing wind. The dust forms and is exposed to strong UV radiation only for a time period of the order of years to hundreds of years, most probably not enough time to form the regular crystal structures of graphite. Alternatively, dust may form relatively far from the nucleus. However, time delay measurements between the optical and

IR band indicate hot dust distances not larger than  $\sim 1$  pc for bright objects (e.g. Sitko et al. 1993, Ulrich, Maraschi & Urry 1997).

The composite 1 spectrum is most probably only weakly reddened, if at all. We estimate this in the following way. We assume that the amorphous carbon grain extinction curve also well represents the reddening within the composite 1 objects. We allow for an arbitrary amount of reddening and compare the resulting spectra with the standard accretion disc spectra of Shakura & Sunyaev (1973). Such models represent bright and blue quasar spectra quite well (see e.g. Koratkar & Blaes 1999 for the discussion of the quasar composite spectrum of Francis et al. 1991).

We can model the composite 1 spectrum assuming any value of  $E_{B-V}$  between 0 and  $\sim 0.05$  by changing the mass and accretion rate of our model. Reddening larger than  $E_{B-V} = 0.05$  is excluded since it leads to an intrinsic spectrum harder than the asymptotic energy index value of 0.33 predicted by the disc model. These two extreme cases of  $E_{B-V} = 0$  and 0.05 are shown in Fig. 2. For all intermediate reddening values the model well represents the overall continuum. However, there is evidently some flattening of the observed spectrum towards IR (see Fig. 2). This effect is well known in AGN although its nature is not clear. It might be caused by the contribution of some starlight in the host galaxy (clearly important for less luminous AGN although not necessarily for bright quasars, see e.g. Elvis et al. 1994), the illumination of the outer disc by the radiation generated in its innermost region, or perhaps some contribution of non-thermal emission to the overall spectrum.

The good correspondence between the dereddened spectrum of the bright quasars with a simple accretion disc model indicates that in these sources the production of X-ray emission does not modify an optically thick flow. In contrast to much fainter Seyfert 1 galaxies, X-ray emission in quasars must therefore make up only a small fraction of the bolometric luminosity. Studies of broad band  $\alpha_{ox}$  index trends with luminosity indeed seem to support such a view (e.g. Bechtold et al. 2003).

## 5 CONCLUSIONS

Analysis of SDSS quasar composites shows that quasar spectra are affected by circumnuclear dust composed primarily of AC amorphous carbon grains. The derived observational extinction curve is similar to SMC extinction but flatter at the shortest wavelengths. Eq. 3 provides a simple empirical formula for the derived quasar extinction law.

## ACKNOWLEDGEMENTS

This work was supported in part by grants 2P03D 003 22 (BCz & ZL) of the Polish State Committee for Scientific Research (KBN). JL acknowledges financial support from the Institute of Physics, Polish Academy of Sciences.

## REFERENCES

Andersen A.C., Sotelo J.A., Niklasson G.A., Pustovit V.N., 2003, *astro-ph/0310343*

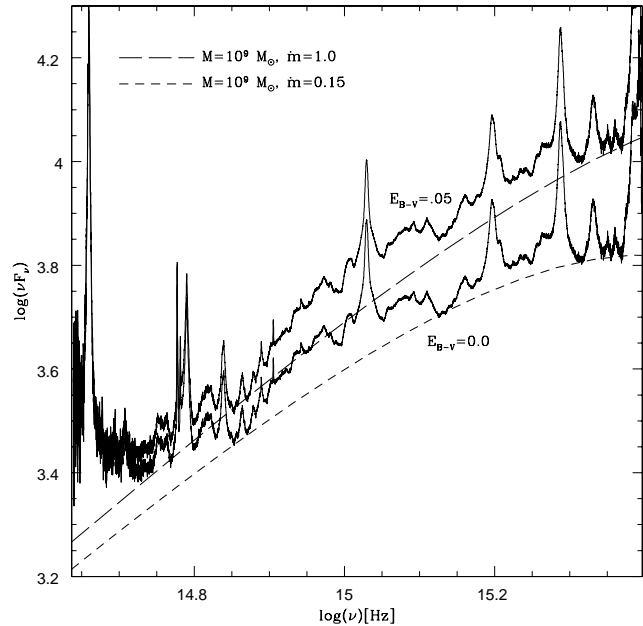


**Figure 2.** The composite 1 of Richards et al. (2003) (lower spectrum) and the same spectrum, but dereddened by  $E_{B-V} = 0.05$  using our AC amorphous extinction curve (upper spectrum). Underlying continua of both spectra can be represented by the the disc spectra models assuming different accretion rates.

- Andreani P., Francheschini A., Granato G., 1999, *MNRAS*, 306, 161  
 Bechtold et al., 2003, *ApJ*, 588, 119  
 Constantin A., Siels J.C., 2003, *astro-ph/0310623*  
 Czerny B., Loska Z., Szczerba R., 1991, in *Physics of Active Galactic Nuclei*, Eds. W.J. Duschl and S.J. Wagner, Berlin:Springer-Verlag, p. 198  
 Czerny B., Loska Z., Szczerba R., Cukierska J., Madejski G., 1995, *Acta Astron.*, 45, 623  
 Dorschner J., Henning T., 1995, *A&ARv*, 6, 271  
 Draine B.T., Lee H.M., 1984, *ApJ*, 285, 89  
 Elvis M., Marengo M., Karovska M., 2002, *ApJ*, 567, L107  
 Elvis et al., 1994, *ApJS*, 95, 1  
 Francis P.J., et al., 1991, *ApJ*, 373, 465  
 Granato G., Danese L., Francheschini A., 1997, *ApJ*, 486, 147  
 Koratkar A., Blaes O., 1999, *PASP*, 111, 1  
 Kuhn O., Elvis M., Bechtold J., Elston R., 2001, *ApJS*, 136, 225  
 Kuraszekiewicz J., Wilkes B.J., 2000, *ApJ*, 542, 692  
 Kuraszekiewicz J., et al., 2003, *ApJ*, 590, 128  
 Laor A., Draine B.T., 1993, *ApJ*, 402, 441  
 Loska Z., Szczerba R., Czerny B., 1993, *MNRAS*, 262, L31  
 Marble A.R. et al., 2003, *ApJ*, 590, 707  
 Mathis J.S., Rumpl W., Nordsieck K.H., 1977, *ApJ*, 217, 425  
 Ogmen M., Duley W.W., 1988, *ApJ*, 334, L1170  
 Omont A., Petijean P., Guilloteau S., McMahon R.G., Solomon P.M., Pecontal E., 1996, *Nature*, 382, 428  
 Piovani L., Tantalò R., Chiosi C., 2003, *A&A*, 408, 559  
 Pitman K., Clayton G.C., Gordon K.D., 2000, *PASP*, 112, 537  
 Prévot M.L., Lequeux J., Prévot L., Maurice E., Rocca-Volmerange B., 1984, *A&A*, 132, 389  
 Priddey R.S., Issak K.G., McMahon G., Robson R.G., Pearson C.P., 2003, *MNRAS*, 344, L74  
 Rawlings J.M.C., Williams D.A., 1989, *MNRAS*, 240, 729  
 Richards et al. 2003, *AJ*, 126, 1131  
 Roche P.F., Aitken D.K., Smith C.H., Ward M.J., 1991, *MNRAS*,

248, 606

Rouleau F., Martin P.G., 1991, ApJ, 375, 526

Seaton M.J., 1979, MNRAS, 187, 785

Shakura N.I., Sunyaev R.A., 1973, A&A, 24, 337

Sitko M.L., Sitko A.K., Siemiginowska A., Szczerba R., 1993, ApJ,  
409, 139

Ulrich M.-H., Maraschi L., Urry M.C., 1997, ARA&A, 35, 445

White R.L. et al., 2003, AJ, 126, 706

This paper has been processed by the authors using the  
Blackwell Scientific Publications L<sup>A</sup>T<sub>E</sub>X style file.